Journal of Physics: Conference Series **630** (2015) 012060 doi:10.1088/1742-6596/630/1/012060

Low Energy Nuclear Structure from Ultrarelativistic Heavy-Light Ion collisions ∗

Enrique Ruiz Arriola[1] **and Wojciech Broniowski**[2,3]

[1] Departamento de Física Atómica, Molecular y Nuclear and Instituto Carlos I de Física Teórica y Computacional, Universidad de Granada, E-18071 Granada, Spain
[2] Institute of Physics, Jan Kochanowski University, 25-406 Kielce, Poland
[3] The H. Niewodniczański Institute of Nuclear Physics PAN, 31-342 Cracow, Poland

E-mail: earriola@ugr.es (ERA)

E-mail: Wojciech.Broniowski@ifj.edu.pl (WB)

Abstract. The search for specific signals in ultrarelativistic heavy-light ion collisions addressing intrinsic geometric features of nuclei may open a new window to low energy nuclear structure. We discuss specifically the phenomenon of α-clustering in ^{12}C when colliding with ^{208}Pb at almost the speed of light.

1. Introduction

Even before the neutron was discovered, based on the α decay explained successfully as a quantum tunneling effect across the Coulomb barrier, Gamow proposed that alpha particles (^{4}He nuclei) are the constituents of atomic nuclei [1]. Indeed, alpha clusters are present in light nuclei (such as, e.g., ^{12}C) as effective degrees of freedom and lead to large intrinsic deformation of their nuclear distributions, which in some cases lead to polyhedral symmetric structures: an equilateral triangle for ^{12}C, tetrahedron for ^{16}O, trigonal bipyramid for ^{20}Ne, octahedron pentagonal bipyramid for ^{24}Mg, hexagonal bipyramid for ^{28}Si, etc. [2, 3, 4, 5, 6], (for reviews see, e.g., [7, 8, 9, 10, 11]).

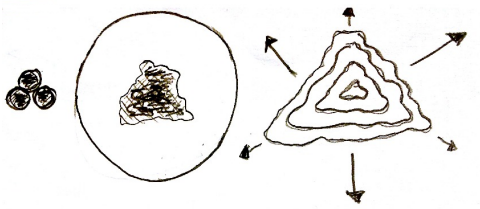

Figure 1. A triangle hitting the wall: ^{12}C pictured as a triangle of three α particles (left) colliding with a heavy ion drawn as a round flat object (middle). The triangular shape of the fireball yields a triangular pattern of particle emission after the collision (right).

∗Talk by ERA at 37th Brazilian Workshop on Nuclear Physics, 8-12 September 2014, Maresias, SP, Brazil

When such a clustered geometric object, say ^{12}C, hits a large nucleus such as ^{208}Pb at almost the speed of light (see Fig. 1), the shape of the created fireball in the transverse plane reflects (up to random fluctuations) the deformation of the light nucleus and effectively implements the almost instantaneous collapse of the collective wave function [12]. As the hit nucleus is large, the fireball is abundant enough to evolve collectively, much as in collisions of two heavy nuclei at RHIC or the LHC. Because of the initial deformation, harmonic flow develops, leading to very specific and measurable signatures in the transverse momentum distributions of the detected hadrons produced in the collision. For instance, the ^{12}C+^{208}Pb system develops large triangular flow, increasing with the multiplicity of the number the produced hadrons. Traditionally, it has been assessed that only some very bulk information on the nuclear structure content could be probed by ultrarelativistic heavy-ion collisions. Our calculations show, however, that certain very distinct geometric features, such as the α-clustering in the nuclear ground state wave function, could indeed be traced significantly by properly analyzing the multiparticle spectrum in the final state [12, 13].

This talk returns to this remarkable link between the lowest energy nuclear structure and the highest-energy heavy-light-ions collisions, emphasizing some important aspects of this connection, mostly from the nuclear physics point of view. This is intended for specialists from either the $\alpha-$cluster and the relativistic heavy-ion communities who might be unfamiliar with the ideas of the other side.

In order to motivate the presentation below, let us review the basic elements needed to describe the collisions between two nuclei, A+B. Let the two nuclei A and B be characterized by wave functions satisfying $H_A\Psi_{n,A} = E_{n,A}\Psi_{n,A}$ and $H_B\Psi_{n,A} = E_{n,A}\Psi_{n,A}$. The collision at invariant CM energy $\sqrt{s}$, in their initial ground state $\Psi_{0,A}$ and $\Psi_{0,B}$, can be described by the total Hamiltonian,

$$H = H_A + H_B + V_{AB}, \tag{1}$$

where additivity of the elementary energy-dependent NN interactions is assumed,

$$V_{AB}(s;\vec{x}_1,\ldots,\vec{x}_A;\vec{y}_1,\ldots,\vec{y}_B) = \sum_{i=1}^{A}\sum_{j=1}^{B} V_{NN}(s,\vec{x}_i-\vec{y}_j), \tag{2}$$

with $V_{NN}(s,\vec{x}) = \mathrm{Re}V_{NN}(s,\vec{x}) + i\mathrm{Im}V_{NN}(s,\vec{x})$ denoting an optical potential. The basic tool of our analysis is given by the Glauber formalism (see, e.g., [14, 15]), which gives the density $P_{AB}(s,\vec{b})$ of inelastic collisions in the transverse plane, $\vec{x} = (\vec{x}_T, z)$, for the A+B reaction in terms of the elementary NN density, $P_{NN}(s,\vec{b})$. For instance, in the binary collision model (the popular wounded nucleon model applied in our studies includes the same ingredients)

$$\begin{aligned} P_{AB}(s,\vec{b}) &= \prod_{i=1}^{A}\int d^3x_i \prod_{j=1}^{B}\int d^3y_j |\psi_{0,A}(\vec{x}_1,\ldots,\vec{x}_A)|^2 |\psi_{0,B}(\vec{y}_1,\ldots,\vec{y}_B)|^2 \\ &\times \frac{1}{\sigma_{AB}^{\mathrm{inel}}(s)}\left\{1-\prod_{i=1}^{A}\prod_{j=1}^{B}\left[1-\sigma_{NN}^{\mathrm{inel}}(s)P_{NN}(s,\vec{b}-\vec{x}_{i,T}+\vec{y}_{j,T})\right]\right\}, \end{aligned} \tag{3}$$

where $\sigma_{NN}^{\mathrm{inel}}(s)$ and $\sigma_{AB}^{\mathrm{inel}}(s)$ are the inelastic cross sections for NN and AB, respectively, and $\int d^2bP_{NN}(s,b) = \int d^2bP_{AB}(s,b) = 1$. This formula shows that we need a knowledge of the nuclear wave functions and the interaction between nucleons in the different nuclei. This is a purely hadronic picture of the collision process and the only partonic underlying features are hidden under $P_{NN}(s,\vec{b})$ which is usually obtained phenomenologically.

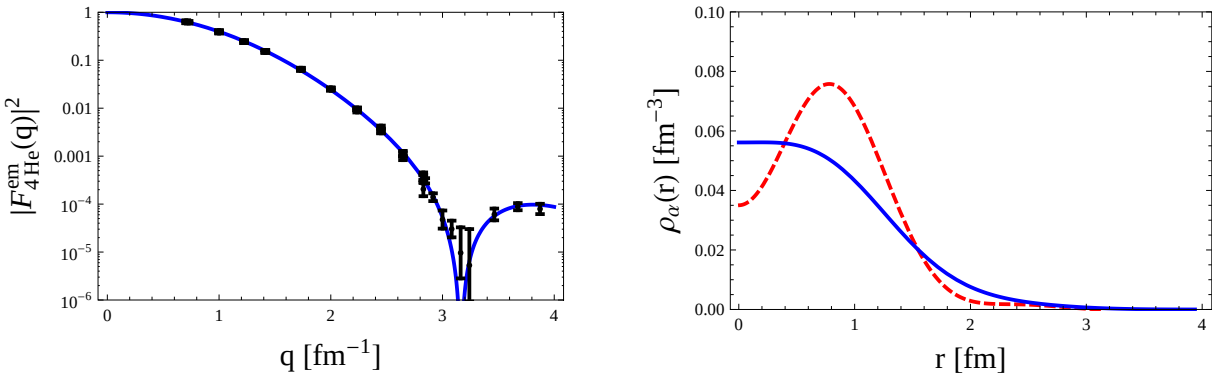

Figure 2. Left: Charge form factor for ^{4}He as a function of the momentum transfer (data from Ref. [16]). Right: Normalized charge (full line) and baryon (dashed line) density for the α particle as functions of the radial distance.

2. The α-particle

2.1. Basic properties

The α particle is a ^{4}He = *ppnn* nucleus, which in the ground state has the quantum numbers $(J^P, T) = (0^+, 0)$. Its charge is $Z_\alpha e = +2e$ and mass $M_\alpha = 2(M_p + M_n) - B = 3727.37$ MeV with the binding energy $B = 28.2957$ MeV. There are no excited states below the $t+p$ or ^{3}He+n thresholds, and the nucleon separation energy is $S_n \sim 20$ MeV. The size information is obtained from the electron scattering, where the elastic $e + ^4$ He differential cross section is given by

$$\left(\frac{d\sigma}{d\Omega}\right)_{e,\alpha} = \frac{d\sigma_{\rm Ruth}}{d\Omega}|F^{\rm em}_{^4{\rm He}}(q)|^2, \tag{4}$$

deviating from the point-like Rutherford result. The charge form factor can be well fitted by [16] $F^{\rm em}_{^4{\rm He}}(q) = \left(1 - q^{12}c^{12}\right) e^{-a^2_{em,\alpha}q^2}$, with $a_{em,\alpha} = 0.681(2)$ fm and $c = 0.316(1)$ fm, and vanishes at $q \simeq 3$ fm, see left Fig. 2. The corresponding charge mean squared radius is $\langle r^2\rangle_{em,\alpha} = 6a^2_{em,\alpha} = (1.668(5)\ {\rm fm})^2$. The nucleon distribution is obtained by unfolding the charge distribution with the nucleon (proton) charge form factor $F^{\rm em}_p(q) = 1/(1 + q^2/\Lambda^2)^2$, $\Lambda^2 = 0.5{\rm GeV}^2$:

$$F^{\rm em}_\alpha(q) = \int d^3x e^{i\vec{q}\cdot\vec{x}}\rho^{\rm em}_\alpha(r) = Z_\alpha F^{\rm em}_p(q)\int d^3x e^{i\vec{q}\cdot\vec{x}}\rho_\alpha(r) \tag{5}$$

and assuming isospin invariance. Then the baryon density $\rho_B(r) = 4\rho_\alpha(r)$. Normalized charge and baryon densities are depicted in right Fig. 2. Thus, we have $\langle r^2\rangle_\alpha = \langle r^2\rangle_{em,\alpha} - \langle r^2\rangle_{em,p} = (1.42\ {\rm fm})^2$.

2.2. Simple wave functions

A good and simple approximation for the wave function in the CM system, as far as the form factor is concerned for $c = 0$ in Eq. (5), is given by the shell model as a $|(1s)^4\rangle$ state,

$$\Psi_\alpha(\vec{x}_1, \vec{x}_2, \vec{x}_3, \vec{x}_4) \;=\; \prod_{i=1}^{4}\frac{e^{-\frac{(\vec{x}_i - \vec{R})^2}{2b^2}}}{(\sqrt{\pi}b)^{3/2}}\mathcal{A}(n\uparrow, n\downarrow, p\uparrow, p\downarrow)\,, \tag{6}$$

where $\mathcal{A}$ is a normalized antisymmetrizer and $\vec{R} = \sum_{i=1}^4 \vec{x}_i/4$ is the CM. The ground state probability $|\Psi_\alpha(\vec{x}_1, \vec{x}_2, \vec{x}_3, \vec{x}_4)|^2$ can be constructed by randomly generating 12 Gaussian variables

describing $\vec{x}_i$ of the four particles, and then relocating the CM $\vec{R} = \sum_{i=1}^{4} x_i/4$ to the origin. More realistic wave functions can be achieved by including a short-distance correlation features, say a hard core of size d, by excluding configurations with $|\vec{x}_i - \vec{x}_j| \leq d$ [17]. This simple approach will be pursued below for the ^{12}C ground state wave function. Further improvements incorporate asymptotic long-distance cluster decomposition conditions on the total wave function into ^{2}H+^{2}H, ^{3}H+n or ^{3}He+p subsystems [18], implying exponential fall-offs with proper separation wave numbers.

3. α-α interaction and effective elementarity

The study of the α-α interaction, involving eight nucleons, has been a continuous playground in cluster model studies [19, 20]. The total wave function is written as $\Psi_{\alpha,\alpha} = \Psi_\alpha(1,2,3,4)\Psi_\alpha(5,6,7,8)\chi_{\alpha\alpha}(r)$, where the relative wave function satisfies a RGM equation containing a direct term which is *local* and corresponds to a folding structure [21] very much like the nucleus-nucleus Sao Paulo potential [22], and an exchange term which is non-local and short range.

3.1. α-α potential

The direct electromagnetic interaction between the two α particles can be written as a folding potential, leading in the overlapping region to the screening of the pure Coulomb interaction below an elementarity radius, r_c,

$$V^{\rm em}_{\alpha\alpha}(r) = \int d^3\vec{r}_1 d^3\vec{r}_2 \frac{\rho^{\rm em}_\alpha(\vec{r}_1)\rho^{\rm em}_\alpha(\vec{r}_2)}{|\vec{r}_1 - \vec{r}_2 - \vec{r}|} = \int \frac{d^3\vec{q}}{(2\pi)^3}\frac{4\pi e^2}{\vec{q}^2}|F^{\rm em}_\alpha(\vec{q})|^2 e^{i\vec{q}\cdot\vec{r}} \sim \frac{Z^2_\alpha e^2}{r}, \qquad r \gtrsim r_c.$$

The leading exchange interaction corresponds to separating one neutron or proton, leaving ^{3}H or ^{3}He behind, respectively, and is $\mathcal{O}(e^{-2\gamma_{n,t}r})$, where $S_n = \gamma^2_{n,t}/(2\mu_{n,t})$ the nucleon separation energy. Using the nuclear form factor, see Fig. 2, we immediately see from Fig. 3 that α particles interact effectively as if they were point-like for distances larger than $r \gtrsim 2.5$ fm. We call this *effective elementarity*, a feature that entitles us to treat interactions between α particles as point-like objects above this separation † and disregard the short-range exchange term. One interpretation of the α clustering is based on the fact that in $A = 4n$ nuclei α particles are on the average packed at a larger distance than r_c, and thus preserve their identity.

3.2. α-α scattering

Assuming this simple picture, we can analyze α-α scattering without much detailed knowledge of the internal α particle structure at sufficiently low energies, with an upper bound fixed by the relative CM momentum $p = \hbar/r_c \sim 200$ MeV corresponding to $T_{LAB} = 2p^2/M_\alpha \sim 15$ MeV. The scattering amplitude is written as a partial wave expansion [25]

$$f(\theta) = f_C(\theta) + \sum_{l=0}^{\infty}(2l+1)e^{2i\sigma_l(p)}\frac{e^{2i\delta_l(p)} - 1}{2ip}P_l(\cos\theta), \tag{7}$$

where $f_C(\theta)$ is the Coulomb amplitude, $\sigma_l(p)$ and $\delta_l(p)$ are the Coulomb and strong phase-shifts, respectively, obtained from solving the relative α-α wave function $\chi_{\alpha,\alpha}(r) \equiv u_{l,p}(r)/r$ with the boundary condition $u_{l,p}(r) \sim G_l(\eta, pr)\sin\delta_l(p) + F_l(\eta, pr)\cos\delta_l(p)$. Here $G_l(\eta, pr)$ and $F_l(\eta, pr)$ are Coulomb wave functions and $\eta = 1/(pa_B)$ is the Sommerfeld parameter and

†Due to the quantum numbers of the α particle, the longest range non-em interaction is of van der Waals nature and is given by Two-Pion-Exchange, a tiny effect [23, 24]. Note that this notion of elementarity has to do with the interaction; the simple overlap integral $\int d^3s\rho_\alpha(s-r)\rho_\alpha(s) \approx 0$ for $r = r_c$ is not the relevant property.

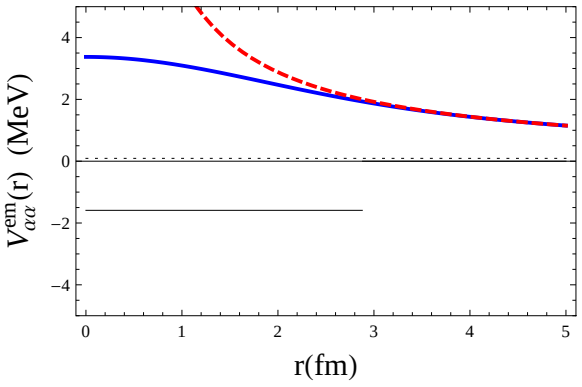

Figure 3. Direct α-α electromagnetic potential (in MeV) as a function of the distance (in fm). We compare the folding potential (solid line) with the elementary Coulomb potential (dashed line), the $Q = 92\,\mathrm{KeV}$ value for ^{8}Be (dotted line) and the $B_{\alpha\alpha} = 1.52$MeV binding when Coulomb is removed above $r_c = 2.88\,\mathrm{fm}$ (solid broken line).

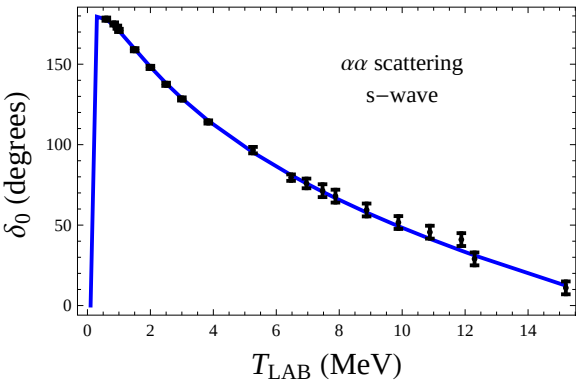

Figure 4. S-wave phase shift for the α-α scattering as a function of the LAB energy. The line is the fit using a boundary condition at a distance of $r_c = 2.88$fm and elementary Coulomb potential above r_c. The data can be traced from Ref. [25].

$a_B = 2/(M_\alpha Z_\alpha^2 e^2) = 3.63\,\mathrm{fm}$ the Bohr radius. Due to the Bose statistics, we have $l = 0, 2, 4, \ldots$. The partial wave expansion, Eq. (7), is limited in practice to $l_{\max} \sim pa$, with a denoting the range of the non-electromagnetic interaction, since classically $L = pb$ and there is no scattering for $b > a$. Below the first inelastic ^{7}Li+p and ^{7}B+n thresholds, which take place at $T_{\mathrm{LAB}} \sim 15$MeV, we have $l_{\max} \sim 4$. Using an energy independent boundary condition at a given cut-off radius r_c we get for $l = 0$ (S-wave)

$$-\frac{1}{M_\alpha}u''_{0,p}(r) + \frac{e^2 Z_\alpha^2}{r}u_{0,p}(r) = \frac{p^2}{M_\alpha}u_{0,p}(r), \qquad L = \frac{u'_{0,p}(r_c)}{u_{0,p}(r_c)}, \tag{8}$$

from which we can fit the S-wave phase-shift with the parameters [23, 24]

$$L = -0.357(3)\ \mathrm{fm}^{-1}, \qquad r_c = 2.88(3)\ \mathrm{fm}, \qquad \chi^2/\mathrm{DOF} = 0.5., \tag{9}$$

which is rather good, see Fig. 4. Thus, all the necessary information is encoded in these parameters, in harmony with an effective elementarity of α particles and the irrelevance of the short distance characteristics. Therefore, as long as α particles remain at distances larger than ~ 3 fm, we may ignore all the substructure details, including the exchange terms. That way one can sidestep a full *ab initio* calculation with 8 nucleons.

3.3. α-α binding and tunneling

The steep rise of the phase-shift starting at zero corresponds to the ^{8}Be resonance, which arises as a pole of the S matrix in the second Riemann sheet. The asymptotics $u_R(r) \to e^{ipr}$ with the complex momentum $p = p_R + \mathrm{i}p_I$ gives a complex energy $E = Q - i\Gamma/2 = (p_R + \mathrm{i}p_I)^2/(2\mu_{\alpha\alpha}) = 92\ \mathrm{KeV} - \frac{\mathrm{i}}{2}3.4(2)$ eV, so that the turning point, fulfilling $Q = V^{\mathrm{em}}_{\alpha\alpha}(r_0)$, is rather large $r_0 = 62$fm, yet tunneling through the barrier occurs. A further interesting aspect is that if the Coulomb force were removed above $r_c = 2.88$ fm, the ^{8}Be resonance would then become a stable weakly bound state with a binding energy given by $B_{\alpha\alpha} = -\gamma_B^2/M_\alpha = -1.5229$ MeV (see Fig. 3), a fairly large radius, $\langle r^2\rangle^{\frac{1}{2}} = 4.0764$ fm, and the asymptotic coefficient of the normalized reduced wave function, $u_B(r) \to A_B e^{-\gamma_B r}$ of $A_B = 2.4163\ \mathrm{fm}^{-1/2}$.

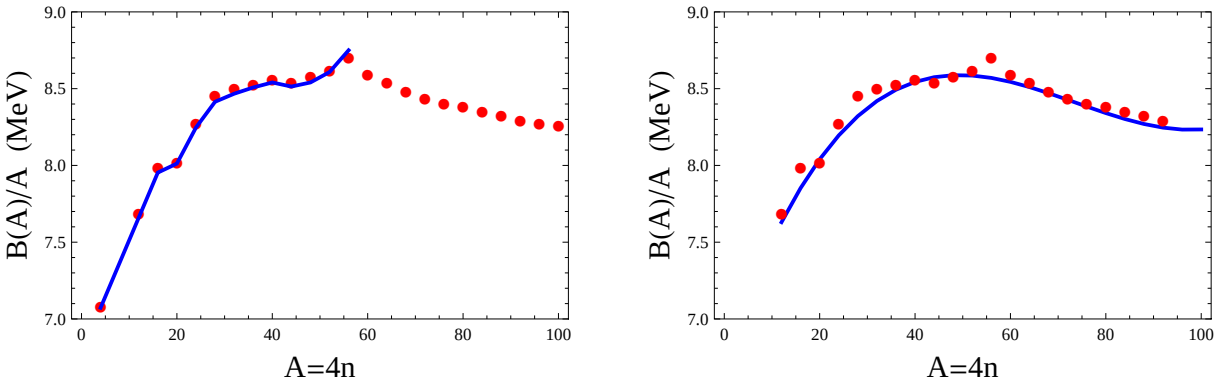

Figure 5. Binding energy per particle as a function of the mass number for $A = 4n$ nuclei. Left: Bonding geometric model. Right: Many-body model containing two-,three- and four-α forces.

4. Evidence for α-clustering

The effective elementarity of α particles has far reaching consequences. The most clear signatures for α clustering in nuclei are seen in the binding energies and form factors. Already in 1966 Harrington proposed to treat ^{12}C as a bound state of three elementary α particles [26].

4.1. Binding energies

Since the α particle is very tightly bound, a hint for clustering for $A = 4n$ nuclei was given by the bonding approximation [3, 27],

$$E(4n) = -B(4n) = -nB_\alpha + n_{\rm bonds}V_{\alpha\alpha} \qquad V_{\alpha\alpha} = -2.29{\rm MeV}\,, \qquad n \geq 3\,, \tag{10}$$

where $n_{\rm bonds} = 3, 4, 8, 12, 16, 19, 22, 25, 27, 30$ for ^{12}C, ^{16}O, ^{20}Ne, ^{24}Mg, ^{28}Si, etc., respectively, yielding $n_{\rm bonds}/n \to 2.5$ (we stop plotting at $A = 56$ since $n_{\rm bonds}$ can always be adjusted onwards). This corresponds a next-neighbors interaction of closely packed spheres (see [7] for pictures illustrating the polyhedral configurations) ‡. The result of the fit can be seen in Fig. 5 (left). One drawback of this approach is that the fit does not reproduce the simplest $n = 2$ case, which corresponds to ^{8}Be.

In a different scheme we just count the numbers of pairs, triplets and quartets, corresponding to two-,three- and four body forces, and the energy reads

$$E(4n) = -nB_\alpha + \left(\begin{array}{c} n \\ 2 \end{array}\right) V_{2\alpha} + \left(\begin{array}{c} n \\ 3 \end{array}\right) V_{3\alpha} + \left(\begin{array}{c} n \\ 4 \end{array}\right) V_{4\alpha}\,, \qquad n \geq 3\,, \tag{11}$$

A fit for $A = 4n$ nuclei gives $V_{2\alpha} = -2.39$ MeV, $V_{3\alpha} = 0.47$ MeV, $V_{4\alpha} = -0.04$ MeV . The result can be seen in Fig. 5 (right), with a mean standard deviation of 0.1 MeV per nucleon. Again, the meaning of $n = 2$ is particularly subtle since, as we have shown, this corresponds to the ^{8}Be case which is unbound by ~ 0.092 MeV while direct extrapolation of the general formula for n implies ~ -2.4 MeV. The ^{8}Be is an exceptionally large system which becomes very sensitive to the long range Coulomb interaction. As we have seen elimination of $V^{\rm em}_{\alpha\alpha}(r)$ above r_c gives $B_{\alpha\alpha} \sim 1.52$ MeV, see Fig. 3, reducing partly the puzzle in the $n = 2$ case both for the bonding model, Eq. (10), and the many body model, Eq. (11).

‡The case of ^{20}Ne would require $n_{\rm bonds} = 9$ for this interpretation but that gives a worse binding.

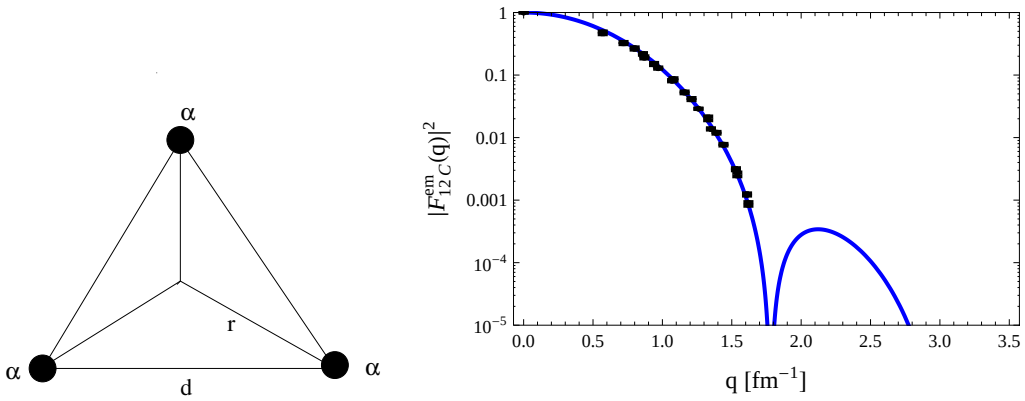

Figure 6. Left: Triangle structure in ^{12}C. Right: Corresponding charge corm factor of ^{12}C from folding the α charge form factor with the triangle $F^{\rm em}_{^{12}C}(q) = F^{\rm em}_{^4He}(q)F_\triangle(q)$ with $d = 3$fm (data from Ref. [28]).

4.2. Cluster Sizes

Charge form factors provide valuable insight on cluster geometries and sizes. If we focus on ^{12}C, we fold an equilateral triangle with side d and radius $r_\triangle = d/\sqrt{3}$ with an α particle, see Fig. 6,

$$F^{\rm em}_{^{12}C}(q) = F^{\rm em}_{^4He}(q)F_\triangle(q)\,, \qquad F_\triangle(q) = \frac{\sin(qd/\sqrt{3})}{qd/\sqrt{3}}\,, \tag{12}$$

A fit to the experimental elastic form factor of ^{12}C [28] taking the experimental $F^{\rm em}_{^4He}(q)$ (see Eq. 5 and Fig. 2) yields $d = 3.05$ fm $> r_c = 2.88$ fm, consistent with the effective elementarity.

4.3. Modeling clustering

Besides this very simple but direct evidence, a massive effort is being carried out [7, 8, 9, 10]) to probe the clusterization features of light nuclei. Clustering in ^{12}C has been described by the Bose-Einstein Condensation (BEC) model [29], the fermionic molecular dynamics (FMD) [30], antisymmetrized molecular dynamics [31], effective chiral field theory on the lattice [32], the no-core shell model [33, 34], or the variational Green's function method (VMC) [35]. The recently discovered 5^- rotational state of ^{12}C in low energy $\alpha+^{12}C$ collisions points to the triangular $\mathcal{D}_{3h}$ symmetry of the system [36]. While it would be best to incorporate realistic calculations (see, e.g., [37, 38]), in Ref. [12] we have applied a simple and practical procedure with α clustered (or unclustered for comparison) random distributions constructed as follows. In the clustered case we randomly generate positions of the 12 nucleons, 4 in each cluster of a Gaussian shape and size r_α. The centers of the clusters are placed in an equilateral triangle of side length d, cf. Fig. 6. The distribution of the 12 nucleons is recentered such that the center of mass is placed at the origin. The short-distance NN repulsion is incorporated by precluding the centers of each pair of nucleons to be closer than the expulsion distance of 0.9 fm [17].

The single and pair distribution functions are defined as (see [40] for multiple distributions)

$$\begin{aligned}
\rho(\vec{x}) &= \langle\Psi_A|\hat{\rho}(\vec{x})|\Psi_A\rangle = \int d^3x_2 \ldots d^3x_A |\Psi_A(\vec{x},\vec{x}_2,\ldots,\vec{x}_A)|^2, \\
\rho_2(\vec{r}) &= \int d^3R d^3x_3 \ldots d^3x_A |\Psi_A(\vec{R}+\frac{1}{2}\vec{r},\vec{R}-\frac{1}{2}\vec{r},\vec{x}_3,\ldots,\vec{x}_A)|^2,
\end{aligned} \tag{13}$$

and are normalized to unity, i.e. $\int d^3r\rho(\vec{r}) = \int d^3r\rho_2(\vec{r}) = 1$, admitting a simple probability interpetation. These are the densities corresponding to point-like nucleons, hence the charge

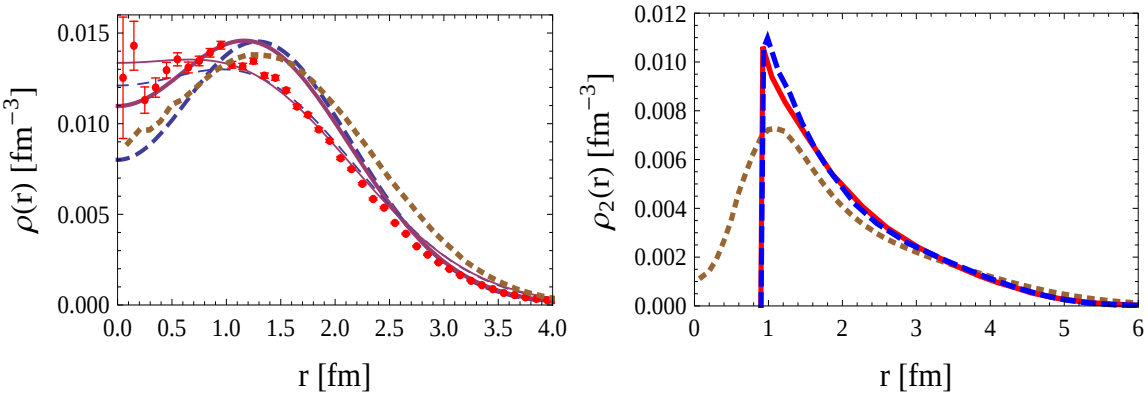

Figure 7. Left: Normalized one-particle distributions in ^{12}C. The electric charge density $\rho^{\rm em}(r)/Z$ (thin lines) and the corresponding distribution of the centers of nucleons $\rho(r)$ (thick lines) in ^{12}C for the data [39] and BEC [29] calculations (dashed lines), FMD [30] calculations (solid lines), and Jastrow correlated wave function [37] (dotted line). Right: Normalized two particle distribution $\rho_2(r)$ in ^{12}C. We show our results for the fitted $\rho(r)$ in the FMD (solid line) and BEC cases (dashed line), and compare to the Jastrow correlated wave function [37] (dotted line).

form factor reads,

$$F_A^{\rm em}(q) = ZF_p^{\rm em}(q) \int d^3x \rho(\vec{x}) e^{i\vec{x}\cdot\vec{q}}, \tag{14}$$

where $F_p^{\rm em}(q)$ is the proton charge form factor (we neglect the small neutron charge form factor and assume isospin symmetry). These densities have exponential fall-offs,

$$\begin{aligned} \Psi_A(\vec{x},\vec{x}_2,\ldots,\vec{x}_A) &\xrightarrow{x\to\infty} Z_A\chi_1(\vec{x})\Psi_{A-1}(\vec{x}_2,\ldots,\vec{x}_A), \\ \Psi_A(\vec{x},\vec{x}',\vec{x}_3,\ldots,\vec{x}_A) &\xrightarrow{x,x'\to\infty} Z_A\chi_{12}(\vec{x},\vec{x}')\Psi_{A-2}(\vec{x}_3,\ldots,\vec{x}_A), \end{aligned} \tag{15}$$

because of the cluster decomposition. In Refs. [18, 41] the calculations explicitly implemented this exact asymptotic property, which would become relevant when separation energies are small or in the case of halo nuclei, which is not the case for ^{12}C in the ground state.

The parameters d and r_α are optimized such that the one particle density $\rho(r)$ of the BEC [29] or FMD [30] calculations are accurately reproduced (as explained, the unfolding of the proton charge density from the charge distribution $\rho^{\rm em}(r)$ is necessary), see Fig. 7. Note a large central depletion in the distributions, originating from the separation of the α clusters. Besides, a fair reproduction of the two-particle densities, $\rho_2(r)$, obtained from multiclustered Jastrow correlated calculations [37] is observed. The radial distribution $4\pi r^2\rho_2(r)$ peaks at the size of the triangle, $d \simeq 3$ fm [42]. Thus, in our simulations we deal with simplified but realistic nuclear distributions of ^{12}C.

5. Ultrarelativistic collisions

We now sketch the basic ingredients behind Eq. (3). We start by analyzing the NN collisions at high energies, where the Mandelstam $s = 4(p^2 + M_N^2)$ in the CM frame.

5.1. NN collisions at high energies

Neglecting spin effects, the scattering amplitude can be written as in Eq. (7) and in the limit $l_{\rm max} \sim pa \gg 1$ we can replace the sum over l by an integral. Using the impact parameter as the

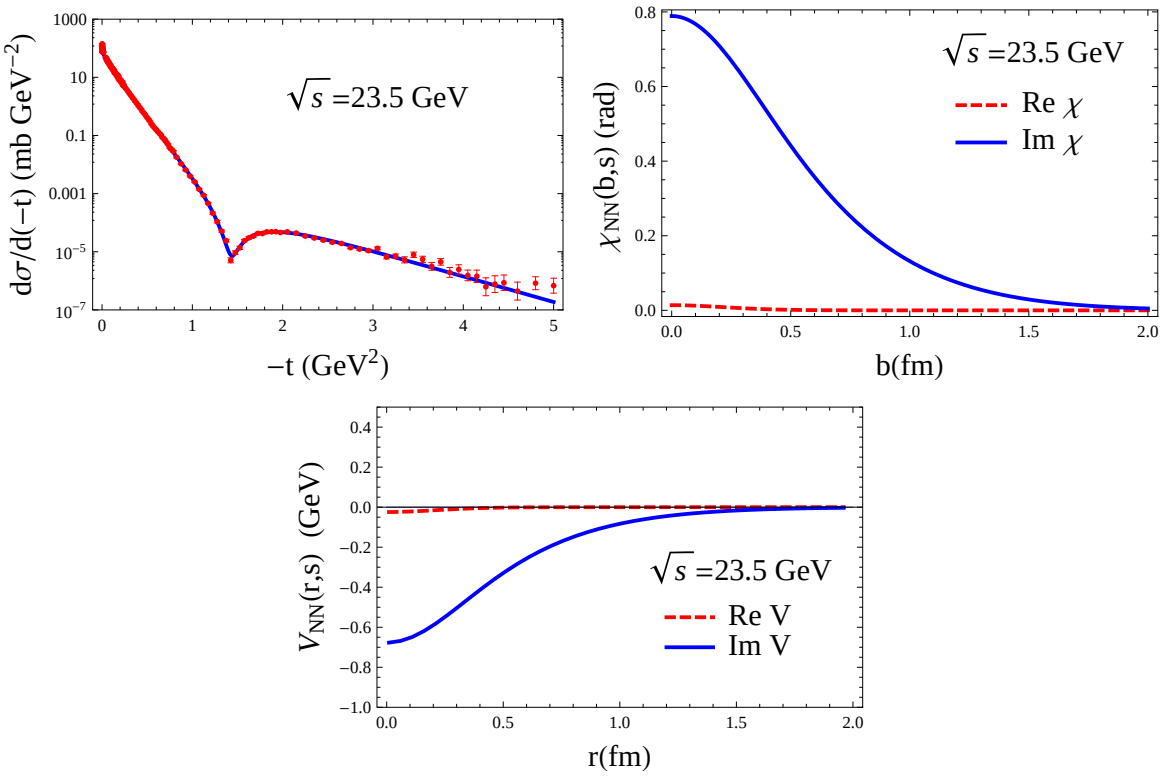

Figure 8. NN scattering at CM energy $\sqrt{s} = 23$ GeV. Top Left: Differential cross section as a function of the invariant squared momentum transfer $-t$ vs. data from [43, 44]. Top Right: Eikonal real and imaginary phase as a function of the impact parameter. Bottom: Optical potential as a function of the distance.

integration variable $b\,p = l + 1/2$, the formula $P_l(\cos\theta) \to J_0(bq)$, and dropping the Coulomb interaction, yields [14]

$$f_{NN\to NN}(s,t) = \frac{ip}{2\pi}\int d^2b[1 - e^{2i\delta(b)}]e^{i\vec{b}\cdot\vec{q}}. \tag{16}$$

At high energies relativistic effects and inelasticities must be taken into account. The general field theoretic approach would require a coupled channel Bethe-Salpeter equation, where the kernel would ultimately be determined phenomenologically from the NN scattering data. Under these circumstances, it is far simpler to use a minimal relativistic approach based on the squared mass operator [45]. Here $\mathcal{M}^2 = P^\mu P_\mu + W$, where W represents the (invariant) interaction determined in the CM frame by matching to the non-relativistic limit with an energy-dependent and local optical potential, $V(\vec{r},s) = \mathrm{Re}V(\vec{r},s) + i\mathrm{Im}V(\vec{r},s)$. This yields for NN after quantization $\hat{\mathcal{M}}^2 = 4(\hat{p}^2 + M_N^2) + 8M_N V$, with $\hat{p} = -i\nabla$, so that the relativistic equation can be written as $\hat{\mathcal{M}}^2\Psi = 4(k^2 + M_N^2)\Psi$, i.e., as a non-relativistic Schrödinger equation

$$(-\nabla^2 + M_N V)\Psi = (s/4 - M_N^2)\Psi\,. \tag{17}$$

In the eikonal approximation the (complex) phase-shift is given by

$$\delta_l(k)\Big|_{l+\frac{1}{2}=bk} \approx -\frac{2\mu}{2k}\int_b^\infty dr\frac{rV(r,s)}{\sqrt{r^2-b^2}} \equiv \frac{1}{2}\chi(b,s) = \frac{1}{2}\mathrm{Re}\chi(b,s) + i\frac{1}{2}\mathrm{Im}\chi(b,s), \tag{18}$$

where $\chi(b,s)$ is the eikonal phase. The optical potential $V(r,s)$ can be obtained from a fit to the experimental elastic differential cross section $d\sigma/d(-t) = |f|^2\pi/p^2$. The fits for pp scattering at $\sqrt{s} = 23.5$ GeV [43, 44] are depicted in Fig. 8 for illustration (details and further results will be presented elsewhere). As we see, both the phase shift and the optical potential are almost purely imaginary, i.e., $\mathrm{Re}\chi(b) \ll \mathrm{Im}\chi(b)$. This is a general feature above $\sqrt{s} \gtrsim 10$ GeV, which allows us to write the inelastic cross section from the optical theorem $\sigma_{\rm tot} = 4\pi \mathrm{Im} f(0)/p \sim \sigma_{\rm inel}$,

$$\sigma_{\rm inel}(s) = \int d^2b \left[1 - e^{-\mathrm{Im}\chi_{NN}(s,b)}\right] \equiv \sigma_{\rm inel}(s) \int d^2b P_{NN}(s,b), \tag{19}$$

in terms of a profile function $P_{NN}(s,b)$ interpreted as the probability of the NN inelastic collision at impact parameter b.

5.2. Nucleus-nucleus scattering (Glauber)

Nucleus-nucleus interactions is most conveniently studied by the Glauber theory applied to multiple scattering (for a review see e.g. [46].), where the highly asymmetric role played by the NN interactions within a given nucleus and NN interactions between nucleons of different nuclei is explicitly exploited. Actually, the interaction time is so short that only high energy states are excited, so basically both incident nuclei remain in their ground states. Under these assumptions, the initial wave function can be written as $\Psi = e^{ipz}\Phi_{AB}\psi_A\psi_B$ for a collision along the $z-$axis, with a slowly varying relative wave function Φ_{AB}. The elastic scattering amplitude becomes

$$f_{AB\to AB}(s,t) = \frac{ip}{2\pi} \int d^2b \langle \Psi_A\Psi_B|[1 - e^{i\chi_{AB}(b)}]|\Psi_A\Psi_B\rangle e^{i\vec{b}\cdot\vec{q}}. \tag{20}$$

The key simplifying aspect is that from the additivity of the NN interactions one obtains the additivity of the eikonal phases,

$$\chi_{AB}(b;\vec{x}_{1,T},\ldots,\vec{x}_{A,T};\vec{y}_{1,T},\ldots,\vec{y}_{B,T}) = \sum_{i=1}^{A}\sum_{j=1}^{B} \chi_{NN}(\vec{b} - \vec{x}_{i,T} + \vec{y}_{j,T}). \tag{21}$$

A purely imaginary NN phase, $\chi_{NN}(b) \sim i\mathrm{Im}\chi_{NN}(b)$, implies a purely imaginary AB-phase, $\chi_{AB}(b) \sim i\mathrm{Im}\chi_{AB}(b)$, and Eq. (3) follows from using again the optical theorem for the AB case.

The evaluation of the Glauber multidimensional integral in Eq. (3), or for the applied wounded nucleon model, can be done through the Monte Carlo techniques such as, e.g., in GLISSANDO [47, 48]. Within such an approach the two-dimensional density of sources can be constructed. We note that a realistic distribution that can be used for the hydrodynamic evolution requires smearing, as to make it sufficiently smooth. We refer to Ref. [12] for illustrations resembling our cartoon of Fig. 1.

Valuable information on the collision geometry and its fluctuations can be obtained from the study of eccentricity parameters (heavily used in relativistic heavy-ion analyses). One introduces the Fourier decomposition of the source density in the transverse plane *in a given event*,

$$\epsilon_n e^{in\Phi_n} = \frac{\int d^2b b^n P(b) e^{in\phi}}{\int d^2b b^n P(b)}, \tag{22}$$

with the eccentricity parameters ϵ_n encoding the information on the shape of the fireball distribution. Here n denotes the rank and Φ_n is the principal axis angle. Then ϵ_2 is called *ellipticity*, ϵ_3 *triangularity*, etc. In general, there are two sources for the ϵ_n parameters: the intrinsic mean deformation of the fireball and fluctuations.

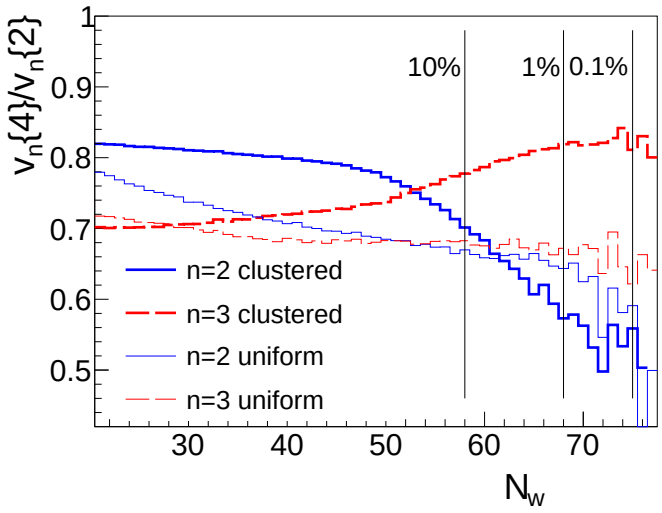

Figure 9. Ratios of harmonic flow coefficients of 4- and 2-particle cumulant moments for the elliptic ($n = 2$) and triangular ($n = 3$) case, plotted as functions of the number of wounded nucleons, and displaying the radically different behavior for the clustered and uniform ^{12}C wave functions (thick vs. thin lines). BEC case, mixed Glauber model for ^{12}C+^{208}Pb collisions with the SPS parameters [13]. The vertical lines indicate centralities.

5.3. Harmonic flow

The harmonic flow consequences, particularly elliptic and triangular flow have been analyzed in detail in Ref. [13, 49], where it is shown that the intrinsic deformation results in very characteristic behavior of the ratios of the so called cumulant moments as functions of the number of participant nucleons, both for the elliptic and triangular deformations. Such ratios are insensitive to the details of dynamics as long as the response of the evolution is linear in the initial deformation, which is the fact for the studied systems [50].

In Fig. 9 we show the ratio of the four- to two-particle cumulant moments for ellipticity and triangularity for the ^{12}C+^{208}Pb collisions at the highest the SPS energy of $\sqrt{s_{NN}} = 17$ GeV. We note a significant difference in the behavior for the clustered wave functions of ^{12}C (thick lines) and the uniform distributions (thin lines). Such effects should be the base for searches of clusterization signals in experiments.

6. Conclusions

When the experimental data on relativistic light-heavy nuclear collisions become available, our method, linking the lowest-energy nuclear phenomena (alpha clustering) and the highest-energy nuclear collisions (collective flow), will offer a novel way to study nuclear correlations in the ground state. Conversely, a detailed knowledge of the clustered light-nucleus wave functions will help to constrain the dynamics of the fireball evolution models (hydrodynamics, transport) and thus gain information on the fundamental properties of the hot and dense matter in the fireball. With this in mind, our method, inherently investigating multiparticle correlations leading to collective effects (harmonic flow), may provide new insights. We stress that since the clusterization phenomenon concerns multi-particle correlations, it is accessible directly only through observables which are many-body. Thus the typically studied one-body quantities, such as excitation spectra of the EM form factors, by definition cannot "prove" clusterization in a direct manner. This unexpected bridge between these two disparate fields of intense activity might enhance the mutual interest of researchers in nuclear structure to produce realistic wave functions which could be used to prepare the initial starting point for the hydrodynamic description of relativistic heavy-ion collisions.

Acknowledgments
This research was supported by the Polish National Science Centre, grants DEC-2011/01/D/ST2/00772 and DEC-2012/06/A/ST2/00390, Spanish DGI (grant FIS2011-24149) and Junta de Andalucía (grant FQM225).

References
[1] Gamow G 1931 *Constitution of atomic nuclei and radioactivity* (Oxford University Press)
[2] Wefelmeier W 1937 *Zeitschrift für Physik* **107** 332–346
[3] Hafstad L R and Teller E 1938 *Phys. Rev.* **54**(9) 681–692
[4] Wheeler J A 1937 *Phys. Rev.* **52**(11) 1083–1106
[5] Brink D 1965 *Proc. Int. School Enrico Fermi, Course* **36**
[6] Brink D, Friedrich H, Weiguny A and Wong C 1970 *Physics Letters B* **33** 143 – 146
[7] Freer M 2007 *Reports on Progress in Physics* **70** 2149
[8] Ikeda K, Myo T, Kato K and Toki H 2010 *Clusters in Nuclei-Vol.1* (Lecture Notes in Physics **818**, Springer)
[9] Beck C 2012 *Clusters in Nuclei-Vol.2* (Lecture Notes in Physics **848**, Springer)
[10] Okolowicz J, Nazarewicz W and Ploszajczak M 2013 *Fortsch.Phys.* **61** 66–79 (*Preprint* 1207.6225)
[11] Zarubin P I 2014 *Clusters in Nuclei-Vol.3* (Springer)
[12] Broniowski W and Arriola E R 2014 *Phys.Rev.Lett.* **112** 112501 (*Preprint* 1312.0289)
[13] Bozek P, Broniowski W, Arriola E R and Rybczynski M 2014 (*Preprint* 1410.7434)
[14] Florkowski W 2010 *Phenomenology of Ultra-Relativistic Heavy-Ion Collisions* (World Scientific Publishing Company, Singapore)
[15] Florkowski W 2014 (*Preprint* 1410.7904)
[16] Frosch R, McCarthy J, Rand R and Yearian M 1967 *Physical Review* **160** 874
[17] Broniowski W and Rybczyński M 2010 *Phys. Rev.* **C81** 064909 (*Preprint* 1003.1088)
[18] Schiavilla R, Pandharipande V and Wiringa R B 1986 *Nucl.Phys.* **A449** 219–242
[19] Tang Y, Lemere M and Thompson D 1978 *Phys.Rept.* **47** 167–223
[20] Friedrich H 1981 *Phys.Rept.* **74** 211–275
[21] Satchler G and Love W 1979 *Phys.Rept.* **55** 183–254
[22] Chamon L, Carlson B, Gasques L, Pereira D, De Conti C *et al.* 2002 *Phys.Rev.* **C66** 014610
[23] Ruiz Arriola E 2007 (*Preprint* 0709.4134)
[24] Ruiz Arriola E 2008 *AIP Conf.Proc.* **1030** 135–140 (*Preprint* 0804.2199)
[25] Afzal S, Ahmad A and Ali S 1969 *Rev.Mod.Phys.* **41** 247–273
[26] Harrington D R 1966 *Phys. Rev.* **147**(3) 685–688
[27] Goldhammer P 1963 *Rev. Mod. Phys.* **35**(1) 40–107
[28] Sick I and McCarthy J 1970 *Nuclear Physics A* **150** 631–654
[29] Funaki Y, Tohsaki A, Horiuchi H, Schuck P and Ropke G 2006 *Eur.Phys.J.* **A28** 259–263
[30] Chernykh M, Feldmeier H, Neff T, von Neumann-Cosel P and Richter A 2007 *Phys.Rev.Lett.* **98** 032501
[31] Kanada-En'yo Y 2007 *Prog.Theor.Phys.* **117** 655–680
[32] Epelbaum E, Krebs H, Lahde T A, Lee D and Meissner U G 2012 *Phys.Rev.Lett.* **109** 252501
[33] Roth R, Binder S, Vobig K, Calci A, Langhammer J *et al.* 2012 *Phys.Rev.Lett.* **109** 052501
[34] Barrett B R, Navratil P and Vary J P 2013 *Prog.Part.Nucl.Phys.* **69** 131–181
[35] Pieper S C, Varga K and Wiringa R B 2002 *Phys.Rev.* **C66** 044310
[36] Marin-Lambarri D, Bijker R, Freer M, Gai M, Kokalova T *et al.* 2014 *Phys.Rev.Lett.* **113** 012502
[37] Buendia E, Galvez F and Sarsa A 2004 *Phys.Rev.* **C70** 054315 (*Preprint* nucl-th/0405027)
[38] Wiringa R, Schiavilla R, Pieper S C and Carlson J 2014 *Physical Review C* **89** 024305 (*Preprint* 1309.3794)
[39] De Vries H, De Jager C and De Vries C 1987 *Atom.Data Nucl.Data Tabl.* **36** 495–536
[40] Viollier R and Walecka J 1977 *Acta Phys.Polon.* **B8** 25
[41] Wiringa R B 1991 *Phys.Rev.* **C43** 1585–1598
[42] Broniowski W and Ruiz Arriola E 2014 (*Preprint* 1407.8495)
[43] Amaldi U and Schubert K R 1980 *Nucl.Phys.* **B166** 301
[44] Amos N A, Block M, Bobbink G, Botje M, Favart D *et al.* 1985 *Nucl.Phys.* **B262** 689
[45] Allen T, Payne G and Polyzou W N 2000 *Phys.Rev.* **C62** 054002 (*Preprint* nucl-th/0005062)
[46] Miller M L, Reygers K, Sanders S J and Steinberg P 2007 *Ann. Rev. Nucl. Part. Sci.* **57** 205–243
[47] Broniowski W, Rybczyński M and Bożek P 2009 *Comput. Phys. Commun.* **180** 69 (*Preprint* 0710.5731)
[48] Rybczyński M, Stefanek G, Broniowski W and Bożek P 2013 (*Preprint* 1310.5475)
[49] Bożek P and Broniowski W 2014 *Phys. Lett. B* **739** 308
[50] Bzdak A, Bozek P and McLerran L 2014 *Nucl.Phys.* **A927** 15–23 (*Preprint* 1311.7325)